

# Electrophoretic Deposition of Latex-Based 3D Colloidal Photonic Crystals: A Technique for Rapid Production of High-Quality Opals

A. L. Rogach,<sup>\*,†,‡,§</sup> N. A. Kotov,<sup>\*,†,||</sup> D. S. Koktysh,<sup>†,‡</sup> J. W. Ostrander,<sup>‡</sup> and G. A. Ragoisha<sup>†</sup>

*Physico-Chemical Research Institute, Belarusian State University, 220050 Minsk, Belarus, Department of Chemistry, Oklahoma State University, Stillwater, Oklahoma 74078, and Center for Laser and Photonics Research, Oklahoma State University, Stillwater, Oklahoma 74078*

*Received March 29, 2000. Revised Manuscript Received June 27, 2000*

Three-dimensional colloidal crystals have been grown by electrophoretic deposition on ITO glass supports from aqueous-ethanol colloidal solutions of monodisperse submicrometer-sized negatively charged polystyrene latex spheres. The technique offers the possibility to produce uniform single-crystal colloidal multilayers on the time scale of minutes, which is a drastic acceleration in comparison with the gravity sedimentation technique that needs weeks or even months. SEM and AFM images of colloidal crystals reveal that close-packed 3D fcc ordering of the latex spheres extends over large areas. Electrophoretically deposited colloidal crystals show a pronounced photonic stopband in the visible spectral range in the normal incidence transmission spectra with a position depending on the size of latex spheres. The electrophoretic deposition has also been used for the impregnation of 3D colloidal crystals with luminescent CdTe nanocrystals. The luminescence spectrum of CdTe nanocrystals shows a dip at the wavelengths corresponding to the spectral position of the photonic stopband of the colloidal crystal.

## Introduction

From the moment of introduction of the photonic band gap concept in 1987 by Jablonovitch and John,<sup>1,2</sup> materials possessing a three-dimensional periodicity of the dielectric constant have been attracting increasing attention. Periodically varying index of refraction in photonic crystals causes a redistribution of the density of photonic states due to the Bragg diffraction, which is associated with stopbands for light propagation. Photonic crystals are potentially interesting in a variety of applications,<sup>3–5</sup> including the inhibition of the spontaneous emission of luminescent species embedded therein in a selected range of wavelengths resulting in the redistribution of emission energy. This effect may serve as a basis for thresholdless lasers.

Periodic structures possessing a photonic band gap in the microwave region were produced by microlitho-

graphic techniques.<sup>6–8</sup> Chemical self-assembly methods have been utilized for making 3D photonic crystals with a photonic band gap in the visible and near-infrared spectral regions.<sup>9–17</sup> Monodisperse silica and latex spheres are the most widely used species for the fabrication of colloidal photonic crystals (artificial opals). Various techniques have been developed for their assembly, including gravity sedimentation on flat<sup>9–12</sup> or periodically patterned<sup>13</sup> substrates, flow of the colloids through micromachined channels<sup>14</sup> or smooth narrow-pore membrane,<sup>15</sup> and making use of capillary forces.<sup>16,17</sup>

- (6) Cheng, C. C.; Scherer, A. *J. Vac. Sci. Technol. B* **1995**, *13*, 2696.
- (7) Wanke, M. C.; Lehmann, O.; Muller, K.; Wen, Q. Z.; Stuke, M. *Science* **1997**, *275*, 1284.
- (8) Lin, S. Y.; Fleming, J. G.; Hetherington, D. L.; Smith, B. K.; Biswas, R.; Ho, K. M.; Sigalas, M. M.; Zubrzycki, W.; Kurtz, S. R.; Bur, A. *Nature* **1998**, *394*, 251.
- (9) Mayoral, R.; Requena, J.; Moya, J. S.; Lopez, C.; Cintas, A.; Miguez, H.; Meseguer, F.; Vazquez, L.; Holgado, M.; Blanco, A. *Adv. Mater.* **1997**, *9*, 257.
- (10) Miguez, H.; Lopez, C.; Meseguer, F.; Blanco, A.; Vazquez, L.; Mayoral, R.; Ocana, M.; Fornes, V.; Mifsud, A. *Appl. Phys. Lett.* **1997**, *71*, 1148.
- (11) Miguez, H.; Meseguer, F.; Lopez, C.; Mifsud, A.; Moya, J. C.; Vazquez, L. *Langmuir* **1997**, *13*, 6009.
- (12) Rogach, O. E.; Kornowski, A.; Kapitonov, A. M.; Gaponenko, N. V.; Gaponenko, S. V.; Eychmüller, A.; Rogach, A. L. *Mater. Sci. Eng. B* **1999**, *64*, 64.
- (13) Van Blaaderen, A.; Ruel, R.; Wiltzius, P. *Nature* **1997**, *385*, 321.
- (14) Park, S. H.; Qin, D.; Xia, Y. *Adv. Mater.* **1998**, *10*, 1028.
- (15) Velev, O. D.; Jede, T. A.; Lobo, R. F.; Lenhoff, A. M. *Chem. Mater.* **1998**, *10*, 3597.
- (16) Denkov, N. D.; Velev, O. D.; Kralchevsky, P. A.; Ivanov, I. B.; Yoshimura, H.; Nagayama, K. *Nature* **1993**, *361*, 26.
- (17) Jiang, P.; Bertone, J. F.; Hwang, K. S.; Colvin, V. L. *Chem. Mater.* **1999**, *11*, 2132.

\* Corresponding authors. E-mails: andrey.rogach@mailcity.com and kotov@okway.okstate.edu.

<sup>†</sup> Belarusian State University.

<sup>‡</sup> Oklahoma State University.

<sup>§</sup> Present address: Institute of Physical Chemistry, University of Hamburg, Bundesstr. 45, D-20146 Hamburg, Germany.

<sup>||</sup> Center for Laser and Photonics Research.

(1) Yablonovitch, E. *Phys. Rev. Lett.* **1987**, *58*, 2059.

(2) John, S. *Phys. Rev. Lett.* **1987**, *58*, 2486.

(3) Joannopoulos, J. D.; Meade, R. D.; Winn, J. N. *Photonic Crystals: Molding the Flow of Light*; Princeton University Press: Princeton, NJ, 1995.

(4) Soukoulis, C. M., Ed. *Photonic Band Gap Materials*; Kluwer: Dordrecht, The Netherlands, 1996.

(5) Special Issue on Electromagnetic Crystal Structures, Design, Synthesis, and Application. *J. Lightwave Technol.* **1999**, *17*.

The most commonly used gravity sedimentation methods require, however, weeks or even months to obtain high-quality colloidal arrays. Electrophoretic deposition has been shown to be a suitable method to induce two-dimensional aggregation of monodisperse metal<sup>18</sup> and latex<sup>19,20</sup> particles. This technique, although being widely employed for the preparation of films of both latex<sup>21</sup> and silica<sup>22–24</sup> particles, was not utilized for the fabrication of ordered 3D colloidal photonic crystals. Very recently, it was demonstrated to accelerate the sedimentation rate of submicrometer-sized silica spheres;<sup>25</sup> however, the quality of the films prepared was not comparable to those obtained by the gravity sedimentation technique. Shortly before the completion of this work, we learned that the electrophoretic deposition was used for the fabrication of micropatterned colloidal assemblies.<sup>26</sup> This paper is focused on solving the problem of tremendous sluggishness of the preparation of the 3D photonic crystals, while maintaining high quality of the assembly. We were able to reduce the time of preparation from months to minutes. Excellent ordering of the crystals is preserved by performing the deposition in a polar yet nonelectroactive dispersion medium. It prevents gas evolution on the electrodes, which is likely to be responsible for structural defects observed in ref 25. The technique presented in this paper has been applied to latex spheres, but can also be successfully used for preparation of silica-based colloidal crystals shown in a separate series of experiments.<sup>27</sup>

It is also of interest to examine the effect of the photonic stopband in the 3D colloidal crystals on the spontaneous emission of light-emitting species embedded therein. One of the most convenient material to use for this purpose is luminescent semiconductor nanocrystals with size-dependent excitonic emission.<sup>28</sup> The 3D colloidal photonic crystals have been filled with luminescent semiconductor nanocrystals by synthesis of CdS and CdSe nanoparticles in opal voids,<sup>29,30</sup> by infiltration of aqueous colloidal solution of CdTe nanoparticles,<sup>31</sup> and by chemical bath deposition of CdS.<sup>32</sup> Here, we demonstrate that the electrophoretic deposi-

tion can also be utilized for the impregnation of 3D colloidal crystals with luminescent CdTe nanocrystals synthesized in aqueous solution. Luminescence spectrum of CdTe nanocrystals exhibits a pronounced dip for the wavelengths that coincide with the spectral position of the photonic stopband of the colloidal crystal.

## Experimental Section

**Materials and Substrates.** Aqueous suspensions of highly monodisperse polystyrene (PS) latex spheres with carboxyl and sulfate groups on the surface (1% aqueous dispersions,  $204 \pm 6$  nm,  $240 \pm 6$  nm,  $269 \pm 7$  nm, and  $300 \pm 5$  nm in diameter) were obtained from Duke Scientific. Ammonium hydroxide (30%) and the pure grade 96% ethanol were purchased from Aldrich. Ultrapure water ( $18.2 \text{ M}\Omega/\text{cm}$ ) was used directly from a Milli-Q water system. Glass slides covered with an ITO layer with a sheet resistance of 8 ohms were received from Delta Technologies. The slides were cut into  $3 \text{ cm} \times 0.5 \text{ cm}$  pieces and used as substrates for electrophoretic deposition.

Aqueous solutions of strongly luminescent CdTe nanocrystals capped with thioglycolic acid (TGA) were prepared by methods reported previously.<sup>33–35</sup> Concentration of CdTe in colloidal solution was 0.013 M referred to Cd.

**Instrumentation.** Direct current power supply (model Topward Electric Ins. Co. Ltd.) was provided by Nomadics Inc. (Stillwater, OK). Absorption and transmission spectra were taken on a HP8453A diode array Hewlett-Packard spectrophotometer. Photoluminescence (PL) spectra were measured on a modular Fluorolog 3 SPEX spectrofluorimeter. Scanning electron microscopy (SEM) pictures were made with a JSM 6400 microscope. Samples for SEM were covered by thin conductive film of gold using Denton Desktop II sputterer (Denton Vacuum Inc.). Atomic force microscopy (AFM) images were taken by using a multimode Nanoscope IIIA instrument (Digital Instruments, CA) operating in the tapping mode with standard silicon nitride tips. Typically, the surface was scanned at 1 Hz with 256 lines per image resolution and 1.2–3.2 V set-point.

**Electrophoretic Deposition.** Electrophoretic deposition of both PS latex spheres and CdTe nanocrystals was performed in a cylindrical glass cell (1 cm diameter) with an ITO glass vertical anode and a stainless steel sheet as a counter electrode connected to a dc power supply through the ammeter. The immersed working area of both electrodes was  $0.5 \text{ cm}^2$ , the distance between electrodes was 0.5 cm. The electrodes were fixed precisely in parallel to each other. Before the deposition, ITO glass substrates were carefully washed under sonication in 1% alconox solution (30 min), pure grade ethanol (30 min), and water (30 min).

Electrophoretic deposition of PS latex spheres has been carried out from the colloidal solution in a water–ethanol mixture. A total of 1 mL of 1% aqueous suspension of colloidal PS latex particles (as purchased from Duke Scientific) was mixed with 44  $\mu\text{L}$  of 30% aqueous  $\text{NH}_4\text{OH}$  solution in ultrasonic water bath, and 2 mL of ethanol was added. The final concentration of PS latex particles was 0.33%, pH of the mixture was 10.5.

A constant voltage of 2 V has been applied to the ITO anode for 30 min to deposit negatively charged PS latex spheres. After the deposition, the coated ITO slides were withdrawn and dried in a glass desiccator over anhydrous calcium sulfate for 1 day.

- (18) Giersig, M.; Mulvaney, P. *J. Phys. Chem.* **1993**, *97*, 6334.  
 (19) Richetti, P.; Prost, J.; Barrios, P. *J. Phys. Lett.* **1984**, *45*, 1137.  
 (20) Böhmer, M. *Langmuir* **1996**, *12*, 5747.  
 (21) Solomentsev, Yu.; Böhmer, M.; Anderson, J. L. *Langmuir* **1997**, *13*, 6058.  
 (22) Nishimori, H.; Tatsumisago, M.; Minami, T. *J. Mater. Sci.* **1996**, *31*, 6529.  
 (23) Hasegawa, K.; Kunugi, S.; Tatsumisago, M.; Minami, T. *Chem. Lett.* **1997**, 1115.  
 (24) Hasegawa, K.; Nishimori, H.; Tatsumisago, M.; Minami, T. *J. Mater. Sci.* **1998**, *33*, 1095.  
 (25) Holgado, M.; Garcia-Santamaria, F.; Blanco, A.; Ibisate, M.; Cintas, A.; Miguez, H.; Serna, C. J.; Molpeceres, C.; Requena, J.; Mijsud, A.; Meseguer, F.; Lopez, C. *Langmuir* **1999**, *15*, 4701.  
 (26) Hayward, R. C.; Saville, D. A.; Aksay, I. A. *Nature* **2000**, *404*, 56.  
 (27) Koktysh, D.; Correa-Duarter, M.; Liz-Marzan, L.; Kotov, N. Unpublished results.  
 (28) Gaponenko, S. V. *Optical Properties of Semiconductor Nanocrystals*; Cambridge University Press: Cambridge, 1998.  
 (29) Romanov, S. G.; Fokin, A. V.; Tretjakov, V. V.; Butko, V. Y.; Alperovich, V. I.; Johnson, N. P.; Sotomayor Torres, C. M. *J. Cryst. Growth* **1996**, *159*, 857.  
 (30) Vlasov, Yu. A.; Luterova, K.; Pelant, I.; Hönerlage, B.; Astratov, V. N. *Appl. Phys. Lett.* **1997**, *71*, 1616.  
 (31) Gaponenko, S. V.; Kapitonov, A. M.; Bogomolov, V. N.; Prokofiev, A. V.; Eychmüller, A.; Rogach, A. L. *JETP Lett.* **1998**, *68*, 142.  
 (32) Blanco, A.; Lopez, C.; Mayoral, R.; Meseguer, F.; Mijsud, A.; Herrero, J. *Appl. Phys. Lett.* **1998**, *73*, 1781.

(33) Rogach, A. L.; Katsikas, L.; Kornowski, A.; Su, D.; Eychmüller, A.; Weller, H. *Ber. Bunsen-Ges. Phys. Chem.* **1996**, *100*, 1772; **1997**, *101*, 1668.

(34) Gao, M.; Kirstein, S.; Möhwald, H.; Rogach, A. L.; Kornowski, A.; Eychmüller, A.; Weller, H. *J. Phys. Chem. B* **1998**, *102*, 8360.

(35) Particles grow continuously during the prolonged refluxing from  $\sim 2.5$  to 5.0 nm. There are hints indicating that the thiols which are initially covalently bound to the particle surface are decomposed by prolonged heat supply and become a sulfide source, so one cannot exclude formation of mixed CdTe(S) crystals under prolonged stages of heating.

CdTe nanocrystals have been deposited from aqueous colloidal solution at pH 10.5 into the pores of previously formed colloidal crystals of PS latex spheres on the ITO supports. The arrangement of the cell was the same as in the case of PS latex deposition. A constant voltage of 2 V was applied for 30 min to deposit negatively charged CdTe nanoparticles on the ITO anodes. After the deposition, the samples were withdrawn and dried in a glass desiccator over anhydrous calcium sulfate for 1 day.

## Results and Discussion

**Preparation and Structure.** Electrophoretic deposition is a process where charged colloidal particles move toward and deposit onto an oppositely charged electrode in a dc field. It has some advantages in the preparation of thick inorganic films such as speed and a possibility to control the film thickness by changing the electro-deposition time.<sup>23</sup> PS latex particles in aqueous suspensions become negatively charged above the isoelectric point at pH  $\sim$  3.5, whereas the complete deprotonation of the surface groups occurs above pH 7.<sup>36</sup> To increase the negative charge of the PS particles, the colloid solution was adjusted to pH = 10.5 by the addition of ammonium hydroxide prior to the electrophoretic deposition. The mobility of the PS colloidal particles has an anomalous dependence on the electrolyte concentration and even increases with the concentration below  $10^{-2}$  M;<sup>37</sup> therefore, the increase in the ionic strength resulting from the pH adjustment did not complicate the migration of the particles to the ITO electrode. However, a problem of carrying out the electrophoretic deposition in aqueous suspension is the decomposition of water, when the bubbles of oxygen formed at the anode penetrate through the deposited compact which would prevent the formation of ordered crystalline arrays of latex spheres. The electrophoretic deposition has been carried out, therefore, from water–ethanol dispersions of PS latex particles, as was done for silica particles in refs 22–24, which allowed the application of a voltage of 2 V without any decomposition of water on electrodes.

The results exceeded our expectations. We obtained brightly colored 10–20 colloidal multilayer samples on the time scale of minutes instead of weeks or even months.<sup>9,11,12</sup> Crystalline quality of colloidal PS latex crystals obtained by electrophoretic deposition has been investigated by SEM and AFM. SEM pictures taken from the top surface show the perfect close-packed order extending over areas of  $\sim 10 \mu\text{m}$  (Figure 1). Two kinds of sphere packing have been observed in the obtained crystals. Both of them are compatible with the face-centered cubic (fcc) structure.<sup>11</sup> Most commonly, we see the hexagonally packed layers of the (111) face of the fcc lattice (Figure 1a). In some areas, the square packed latex spheres, which correspond to the (100) face of the fcc structure, can be found (Figure 1b). The switching from (111) to (100) plane of growth is likely to be influenced by the roughness of the ITO substrate (Figure 2a). Although it is rather small—in the range of 60 nm—yet it is comparable with the size of the latex spheres. A local distribution of hills and valleys augmented by the electrical field on conductive ITO sub-

strate may randomly favor the cubic 2D ordering of the latex particles, which continues to grow this way further. Rarity of the (100) packing suggests that the surface topography prompting the nucleation of the cubic face is a quite atypical statistical event.

The perfect fcc crystalline order extends uniformly in the direction perpendicular to the substrate over the entire film thickness when looking at the stacking edges (Figure 1c,d), which is especially important for the optical properties of colloidal crystals. We did not observe terraces at the cleaved edges of the samples which is a common issue for colloidal crystals grown by the sedimentation technique.<sup>11</sup>

The fcc structure has a preference over the hexagonal-close-packed (hcp) structure due to a slight difference in the energy of hard sphere stacking in the fcc and hcp arrangement as shown in the calculations of Woodcock.<sup>38</sup> Although the preferential fcc structuring has been observed for colloid crystals formed by sedimentation,<sup>11</sup> it was not obvious that the small energetic difference should be significant enough for the electrophoretic deposition, because the sedimentation is a much slower and reversible process. Our experiments show that even at high sedimentation rates that are characteristic for the electrophoretic deposition, the crystallization is still energetically selective.

When looking at the SEM images at lower magnification (Figure 1e,f), two types of defects are routinely observed. The first one is sphere vacancies appearing every  $\sim 10 \mu\text{m}$  on average. Note that no single sphere lying on the top surface was observed over the entire top layer of the samples. They represent a structural feature typically encountered in gravity-sedimented colloidal crystals. The second type of defect is vertical cracks perpendicular to the substrate. They were observed every  $\sim 10 \mu\text{m}$  and usually did not disturb the fcc order in the films. The reason for their appearance is most probably the deposition of Au and the subsequent high vacuum exposure of the samples in the SEM, and/or drying-induced shrinkage.<sup>17,39</sup> Interestingly, the crystalline packings on both sides of the gap are always complementary to each other. This indicates that the film maintains continuity as it grows, whereas cracking occurs at the SEM sample preparation stage.

AFM images made in the tapping mode from the top surface show, again, good fcc packing with a long-range order (Figure 2b). This is also illustrated by the two-dimensional Fourier transform (inset to Figure 2b). The vertical cracks were hardly observed at all when AFM was used for characterization of the surface of the same samples. The same observation has been done in ref 17 for colloidal crystals made from uniform silica spheres.

The features discussed above were characteristic for PS latex spheres of all diameters used in this study. The only difference was a smaller number of vertical cracks observed in SEM for colloidal crystals made from larger latex particles.

The force guiding the latex particles to the substrate is much stronger in the case of electrophoretic deposition than in gravitational sedimentation. This promotes the overall quality of the film and the preferential orientation of the colloidal crystal. Added alcohol—besides

(36) Donath, E.; Walther, D.; Shilov, V. N.; Knippel, E.; Budde, A.; Lowack, K.; Helm, C. A.; Möhwald, H. *Langmuir* **1997**, *13*, 5294.

(37) Folkersma, R.; Van Diemen, A. J. G.; Stein, H. N. *Langmuir* **1998**, *14*, 5973.

(38) Woodcock, L. V. *Nature* **1997**, *385*, 141.

(39) Skjeltorp, A. T.; Meakin, P. *Nature* **1988**, *335*, 424.

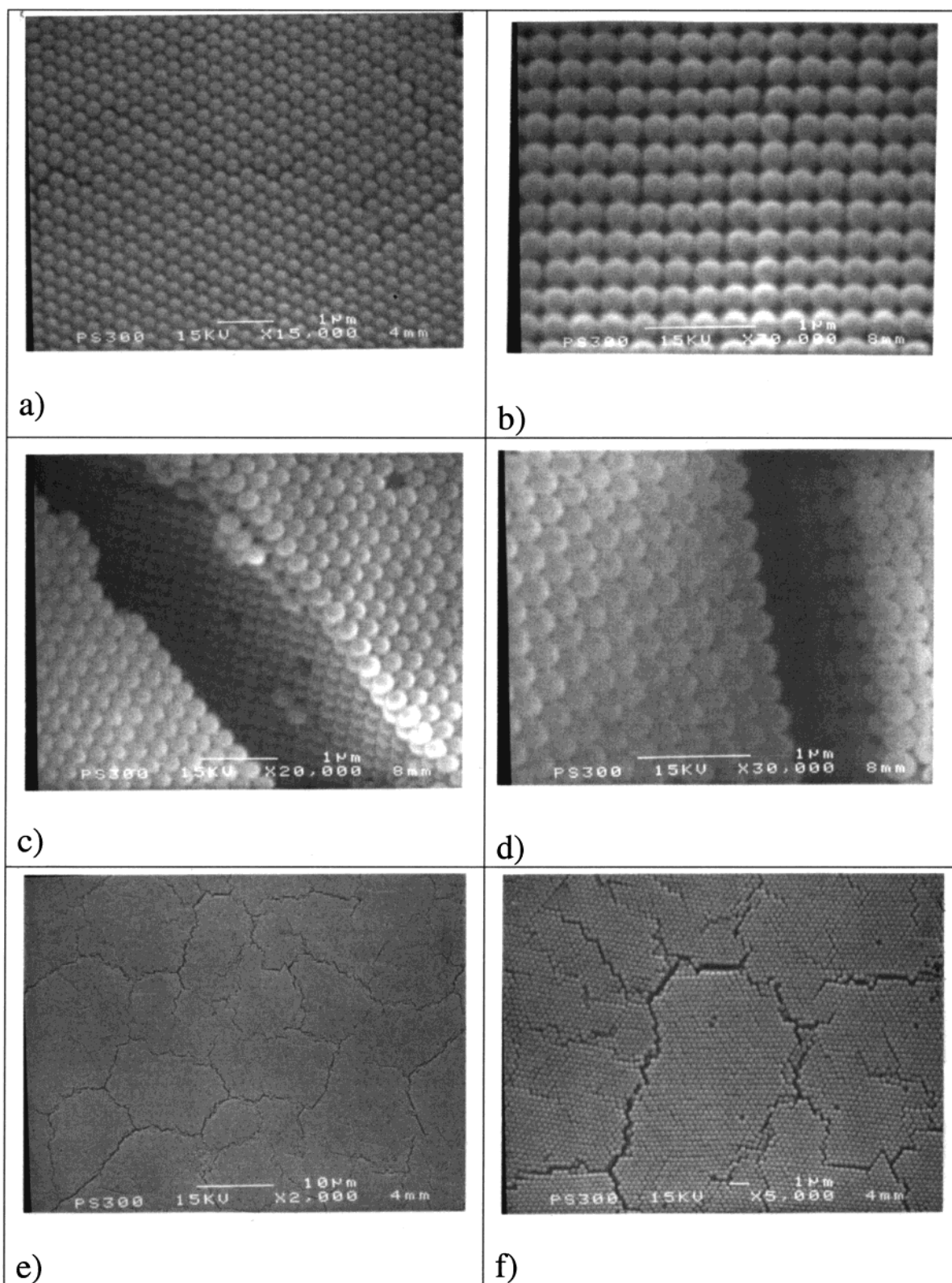


**Figure 1.** SEM images of top (a, b, e, and f) surface and cleaved edges (c and d) of a colloidal crystal made from 300 nm PS latex spheres. Both high- (a and b) and low-magnification (e and f) pictures of the surface are shown.

preventing the gas evolution—reduces the dielectric constant of the medium, which also contributes to greater attractive force between the colloid and the electrode. We believe that it also improves the crystal packing as compared with the deposition from water.<sup>25</sup>

**Optical Properties.** Colloidal crystals made from PS latex spheres were brightly colored in both transmitted

and reflected light because of the optical diffraction on regular multilayers. Optical transmission spectra of the samples measured at normal incidence (the angle between the light propagation vector and surface normal  $\theta = 0^\circ$ ) show an existence of a pronounced photonic stop band (Figure 3) due to the Bragg reflection on the (111) planes. The position of this band changes systematically

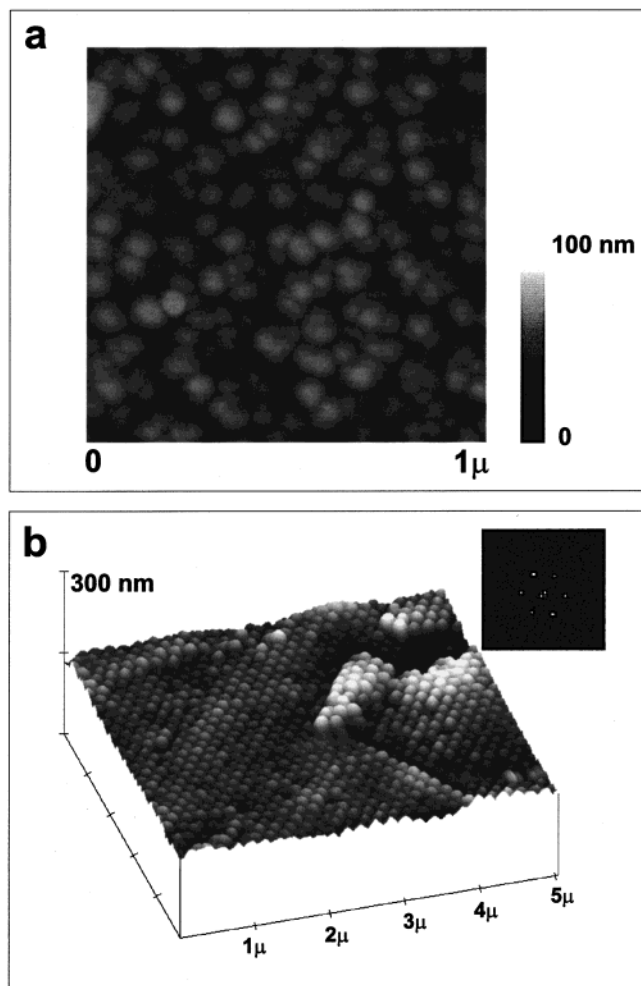


**Figure 2.** (a) Tapping mode AFM image of a surface of ITO substrate and (b) 3D tapping mode AFM image of a surface of a colloidal crystal made from 204 nm PS latex spheres. The inset shows a Fourier transform of a  $2 \times 2 \mu\text{m}^2$  region.

with size of latex spheres according to the following equation:<sup>10</sup>  $\lambda_c = 2n_{\text{eff}}d$ , with  $n_{\text{eff}}^2 = n_{\text{latex}}^2f + n_{\text{air}}^2(1 - f)$ , where  $n_{\text{eff}}$  is the effective refractive index of the latex/air composite;  $f = 0.74$  is the filling factor for a close packed structure;  $d = (2/3)^{1/2}D$  the distance between crystalline planes in the direction  $\theta = 0^\circ$ ;  $D$  is the sphere diameter. Thus, the position of the dip in the transmission can be tuned accurately through the particle size control. Figure 4 shows the experimental dependence of the position of the stop band minimum  $\lambda_c$  in the transmission spectra of colloidal crystals on the diameter  $D$  of the PS latex spheres and a theoretical fit to the Bragg law (with  $n_{\text{latex}} = 1.59$ ). The calculated line lies higher than the fit to experimental points. This discrepancy could be caused by the shrinkage of latex particles during the drying, so that their effective diameter differs from that in aqueous suspensions. It corresponds to  $\sim 5.0\%$  of decrease in the sphere size for the smallest and  $6.3\%$  for the largest latex spheres used. The shrinkage of latex spheres<sup>39</sup> could be also responsible for the appearance of vertical cracks through the colloidal crystals as mentioned above.

**Impregnation with CdTe Nanocrystals.** The voids of the electrophoretically prepared 3D colloidal photonic crystals can be filled with CdTe nanocrystals using the electrophoretic technique similar to the technique that

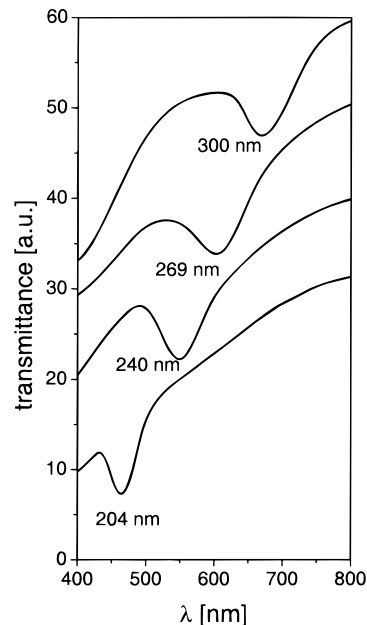


**Figure 3.** Normal incidence transmission spectra of colloidal crystals made from PS latex spheres of different sizes (shown on the picture).

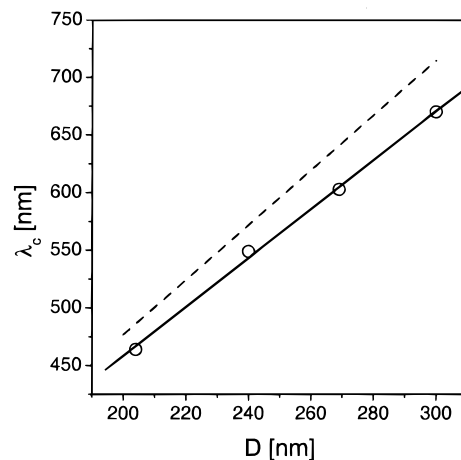


**Figure 4.** Experimental dependence of the position of the stop band minimum  $\lambda_c$  in the transmission spectra of colloidal crystals on the diameter  $D$  of the PS latex spheres (circles and solid line fit) and a theoretical fit to the Bragg law (dashed line).

was recently applied for the deposition of CdTe nanocrystalline thin films on ITO substrates.<sup>40</sup> CdTe nanoparticles in aqueous colloidal solutions show pronounced 1s–1s electronic transitions in the absorption spectra and a relatively narrow (fwhm = 45 nm) and strong (up to 20% room-temperature quantum efficiency as measured in comparison with Rhodamine 6G) “excitonic” PL which is tunable with particle size due to the quantum confinement effect (Figure 5). TGA-stabilized CdTe nanocrystals of 3.5–4.5 nm size have favorable conditions for migration in the electric field both in the colloidal solution and in the channels formed by the voids in the colloidal crystal due to a low mass and diameter and the negative charge resulting from the charged functional groups of TGA. The electrophoresis

(40) Ragoisha G. A. In *Physics, Chemistry and Application of Nanostructures*, World Scientific Publishing: Singapore, 1999; p 193.

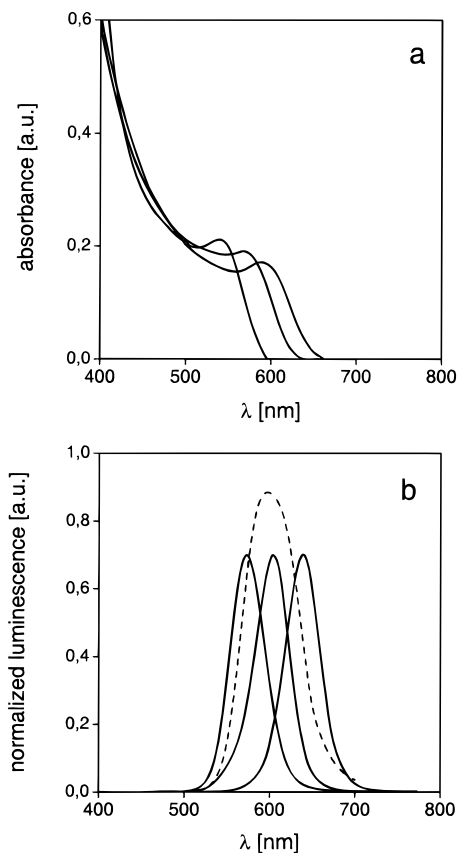


**Figure 5.** Absorption (a) and luminescence (b) spectra of TGA-capped CdTe nanocrystals of different sizes (3.5–4.5 nm) in aqueous solutions. Luminescence spectrum of a mixture of CdTe nanoparticles of different sizes is also shown (panel b, dashed line).  $\lambda_{\text{ex}}$  is 400 nm in all cases.

in CdTe nanocolloid solution is much like the common electrolysis, i.e. the rate of the electrostimulated process is high and can be controlled by the potential in the range of common electrochemical reactions.<sup>40</sup> The ability of CdTe nanocrystals to deposit on the anode at low potentials and penetrate through the PS colloid crystal appeared to be dependent on the pH. Although an alkaline medium favored migration of the CdTe nanocrystals in the electric field due to their negative charging attributed to the deprotonation of TGA, the optimal conditions were found to be at pH = 10.5, being determined by the interplay of the electrophoretic force and the electrostatic repulsion from the negatively charged latex particles. Further increase in the pH complicated CdTe deposition by the competing anodic reactions.

To investigate the influence of the photonic band gap of a colloidal crystal on the luminescence of CdTe nanocrystals embedded therein, we used a mixture of CdTe nanoparticles of different sizes which gave a broad PL spectrum centered at around 600 nm (Figure 5, dashed line) for impregnation of the colloidal crystal made from PS latex globules of 269 nm size. The luminescence spectrum of CdTe nanocrystals changes when it overlaps with the optical stopband of the colloidal crystal (Figure 6). We observed a dip in the emission spectrum correlating with the spectral position of the stopband, i.e. the inhibition of spontaneous emission of semiconductor nanocrystals as a result of a

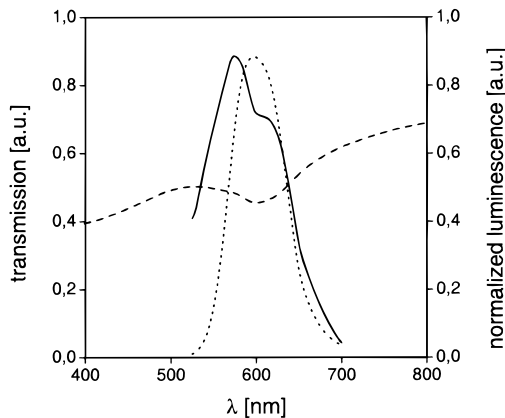


**Figure 6.** Modification of the spontaneous emission of CdTe nanocrystals embedded in a colloidal crystal. Luminescence spectrum of CdTe nanocrystals electrophoretically deposited into the voids of colloidal crystals made of PS latex globules of 269 nm (solid line) shows a dip correlating with the spectral position of the stopband in the transmission spectrum of the colloidal crystal (dashed line). Luminescence spectrum of CdTe nanoparticles in aqueous solution is also shown (dotted line).  $\lambda_{\text{ex}}$  is 400 nm in all cases.

modified photon density of states within this spectral region.<sup>31,32</sup>

## Conclusions

The electrophoretic deposition technique produces single-crystal colloidal multilayers on the time scale of minutes, which is a drastic acceleration in comparison with the most common gravity sedimentation technique. It is also quite simple in realization and yields 3D photonic crystals of quality comparable of higher than the other methods. We envision it to be applicable to a wide variety of particles; however, it is necessary to note that the colloids to be deposited should be tolerant to the addition of alcohol to the dispersion.

Besides acceleration, the electrophoretic deposition offers the possibility of patterning<sup>26</sup> and impregnating of the photonic crystals with luminescent materials. This technique also opens the possibility of preparation of uniform coatings from photonic crystals on curved substances such as spheres, which would be impossible by means of gravitational or centrifugal forces. Such coatings can be the basis of unique diffraction optic devices. The overlap of the photonic stopband and the spectrum of spontaneous emission of the impregnated species results in the redistribution of the emission energy in such system. This phenomenon represents both fundamental and practical importance for the design of photonic devices.

**Acknowledgment.** The Belarusian team has been supported in part by research grant INTAS-Belarus 97-250. N.A.K. thanks NSF-CAREER, AFSOR, OCAST and Nomadics Inc. for partial financial support of this research. A.L.R. and N.A.K. acknowledge the support of the National Research Council (COBASE grants program) that made collaborative work on this project possible. N.A.K. and D.S.K. acknowledge the research scholarship (DGE-9902637) from the NSF-NATO.